

Unlocking Low-Light-Rainy Image Restoration by Dual Degradation Feature Guidance

Xin Lin¹, Jingtong Yue¹, Sixian Ding¹, Chao Ren¹, Chun-Le Guo², Chongyi Li^{2,3}

¹Sichuan University, Chengdu, China

²Nankai University, Tianjin, China

³Nanyang Technological University, Singapore, Singapore

linxin@stu.scu.edu.cn, yuejingtong137@gmail.com, dingsixian@stu.scu.edu.cn,

chaoren@scu.edu.cn, guochunle@nankai.edu.cn, lichongyi25@gmail.com

Abstract

Rain in the dark is a common natural phenomenon. Photos captured in such a condition significantly impact the performance of various nighttime activities, such as autonomous driving, surveillance systems, and night photography. While existing methods designed for low-light enhancement or deraining show promising performance, they have limitations in simultaneously addressing the task of brightening low light and removing rain. Furthermore, using a cascade approach, such as “deraining followed by low-light enhancement” or vice versa, may lead to rain patterns that is difficult to handle or excessively blurred and overexposed images. To overcome these limitations, we propose an end-to-end network called $L^2RIRNet$ which can jointly handle low-light enhancement and deraining in real world. Our network mainly includes a Pairwise Degradation Feature Vector Extraction Network (P-Net) and a Restoration Network (R-Net). P-Net can learn degradation feature vectors on the dark and light areas separately, using contrastive learning to guide the image restoration process. The R-Net is responsible for restoring the image. We also introduce an effective Fast Fourier - ResNet Detail Guidance Module (FFR-DG) that initially guides image restoration using detail images which do not contain degradation information but focus on texture detail information. Additionally, we contribute a dataset containing both synthetic and real-world low-light-rainy images. Extensive experiments demonstrate that our $L^2RIRNet$ outperforms the existing methods in both synthetic and complex real-world scenarios. Code and dataset will be released.

Introduction

Low-Light-Rainy (LLR) condition presents a significant challenge for the tasks of autonomous driving, surveillance systems, and photography. Rain pattern information is difficult to be captured, particularly in low-light conditions, while low-light areas are also difficult to be achieved due to the presence of rain patterns. The joint task of low-light image enhancement and deraining is common yet challenging.

Motivation Although existing single image rain removal (SIRR) and low-light enhancement (LLE) methods have significantly progressed in handling corresponding image

degradation, they are limited in solving the joint task. Cascading two single-task networks still cannot achieve satisfactory results. As shown in Figure 1(b), the low-light enhancement method SCI can only improve the light intensity and make the rain pattern in the dark areas more visible but cannot remove rain from images. In Figure 1(c), the deraining method RCDNet, which is trained on the (Fu et al. 2017b) dataset, only considers daytime scenes, making it challenging to remove the rain patterns in the dark areas, and the background information in dark areas remains unavailable. In Figure 1(d) and 1(e), combining state-of-the-art low-light enhancement and deraining networks (SCI and RCDNet), it still presents issues such as over- or under-exposure in certain areas and difficulties in removing specific rain streaks. Therefore, it is essential to propose a network that can simultaneously enhance light and remove rain to address the limitations of existing solutions.

In this study, we propose a unified Network for Low-Light-Rainy Image Restoration ($L^2RIRNet$), which can simultaneously enhance light and remove rain streaks with high efficiency. $L^2RIRNet$ consists of two main components: a Pairwise Degradation Feature Vector Extraction Network (P-Net) and a Restoration Network (R-Net). The P-Net extracts the degradation feature vector from low-light-rainy images and learns it separately. This structure allows learning more accurate degradation information based on the distribution characteristics of low-light-rainy images. The targeted extraction of the degradation feature vector is then used to guide the image restoration process carried out by R-Net, which considers real-world factors that affect the image quality. Additionally, we introduce a simple yet effective module, the Fast Fourier ResNet Detail Guidance Module (FFR-DG Module). We obtain a detail image by subtracting the three channels of the image from each other and concatenating them. The detail image reduces the effect of rain pattern information and retains the detailed texture information of the original image, which guides the subsequent restoration process skillfully. Extensive experiments show that the FFR-DG has a significant impact on the performance of our method. To train our model, we also build a dataset consisting of two parts, synthesized image pairs and real-world images. Our contributions can be summarized as follows:

- We propose a novel $L^2RIRNet$ that simultaneously performs low-light enhancement and deraining. Our exten-

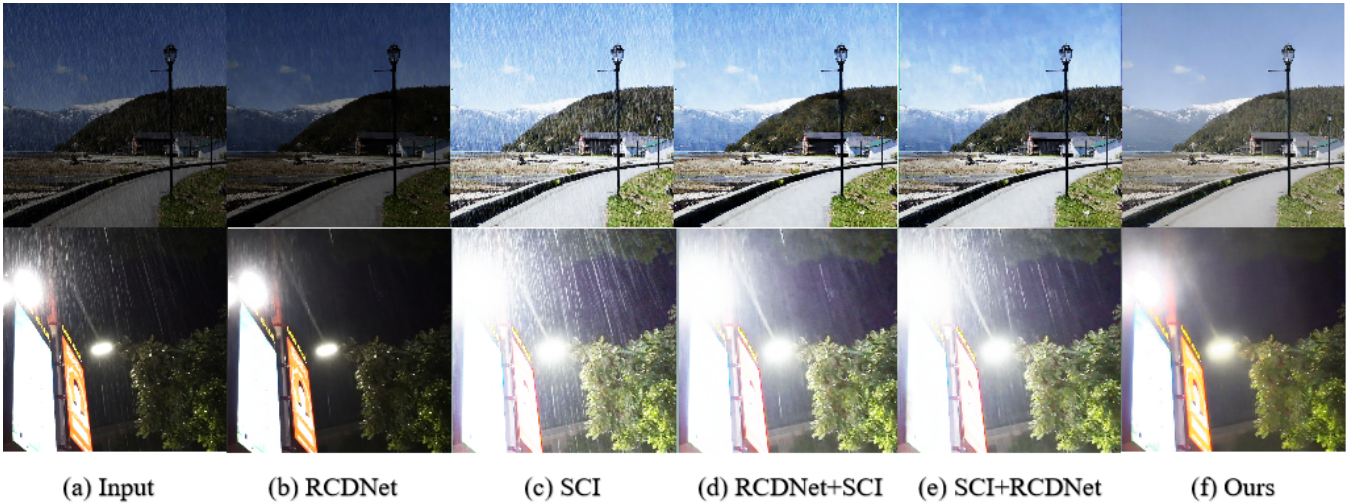


Figure 1: We compare the performance of existing low-light enhancement and deraining methods on both synthetic (1st row) and real-world (2nd row) low-light-rainy images. The results reveal that these methods struggle to handle low-light-rainy conditions. (a) Input; (b) RCDNet; (c) SCI; (d) RCDNet + SCI; (e) SCI + RCDNet; (f) $L^2RIRNet$ (Ours). While single-task networks can only address either low-light enhancement or deraining, the cascaded methods may lead to overexposure, underexposure, residual rain patterns, and blurring. In contrast, our $L^2RIRNet$ can achieve simultaneous low-light enhancement and deraining.

sive experimental results show that our method outperforms the existing methods on both synthetic and real images.

- The degradation feature vector in low-light-rainy images is inconsistent across the image. Thus we present a P-Net that employs shared encoders to learn different types of degraded feature vectors separately. This design provides better guidance than using a single branch for restoration.
- We introduce an R-Net built on the proposed FFR-DG module. The FFR-DG module explores the texture detail image with spatial and frequency domain information to provide effective prior guidance for the image restoration process in the R-Net.

Related Work

Single Image Rain Removal. Image deraining is a challenging problem due to its ill-posed nature. Traditional methods aim to reconstruct the background from a rainy image by extracting the high-frequency part (HFP) stripped of rain. This can be achieved through various filtering strategies such as guided filters (Jing et al. 2012), multiple guided filtering (Zheng et al. 2013), and nonlocal means filtering (Kim et al. 2014). For deep learning based methods, Fu et al. (Fu et al. 2017a) proposed a CNN that could extract discriminative features of rain in the HFP of a single rainy image. A new research direction is to use high-level semantic information to improve rain removal (Wei et al. 2022b). In addition, some researchers focus on more complex task settings, such as synchronous rain streaks and raindrop removal (Wei et al. 2022a). (W et al. 2022) proposed a novel feature extraction network, which is effective in both image restoration and enhancement. (Wang et al. 2023) introduced an unfolding method, through multi-stages training M-net

and B-net to achieve superior performance in image deraining. All of these methods can only restore the rain images captured in daytime, and they cannot remove rain patterns well in the low-light condition.

Low-light Image Enhancement. In order to enhance low-light images, traditional methods have utilized handcrafted optimization techniques and norm minimization methods. These methods make use of various assumptions such as dark/bright channel priors (Guo, Yu, and Ling 2016; Fu et al. 2013; Zhihong and Xiaohong 2011) and mathematical models such as retinex theory (C. et al. 2018) and Multi-scale Retinex theory (Rahman, Jobson, and Woodell 1996; Jobson 2004) to obtain sub-optimal solutions. The learning-based methods can be divided into four categories: supervised (Fu et al. 2013), self-supervised (Ma et al. 2022), unsupervised (Y, X, and D 2021), zero-shot (Guo et al. 2020). These methods can be broadly categorized into two approaches: end-to-end and theoretical schemes such as retinex decomposition. (Zhang, Zhang, and Guo 2019) considered the effects of the noise in low-light images and proposed a noise removal module that improves the performance of the network. Zero-shot approaches propose different approximation strategies to reduce label dependency. Zero-DCE (Guo et al. 2020) and Zero-DCE++ (Li, Guo, and Loy 2021) estimated multiple tone-curves from input images to obtain enhanced images. SCI (Ma et al. 2022) created a self-supervised framework by implementing a cascaded illumination learning approach. This helps minimize redundancy and enhance the overall efficiency of the process. PyDiff (Zhou, Yang, and Yang 2023) is the first to consider diffusion model in low-light enhancement, and achieves better performance and speed than existing methods. However, for low-light-rainy images, these methods only enhance the brightness and make the rain patterns more visible in the dark areas, but cannot restore the

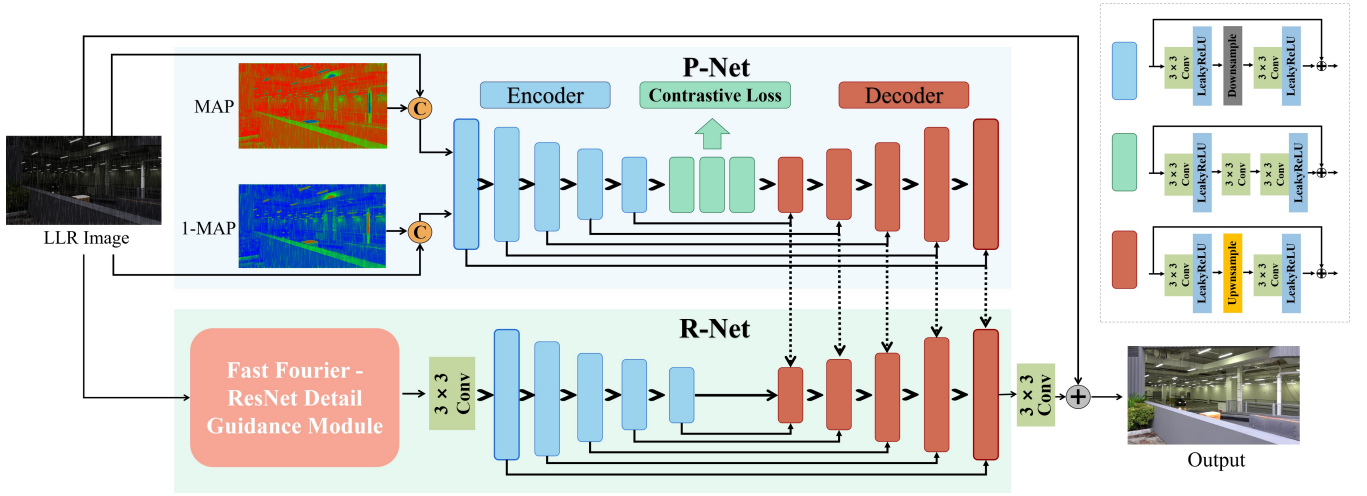


Figure 2: The architecture of the proposed $L^2RIRNet$ framework consists of two parts: a P-Net and an R-Net, both of which are based on the design of U-Net. P-Net is responsible for extracting the degradation feature vector of both bright and dark regions of the image using attention and its complementing map, respectively. The encoder then learns the loss constraint by comparing these two feature vectors. The decoder generates the multi-channel latent features, which guide the restoration process. R-Net is responsible for restoring the image. The preprocessing of the low-light-rainy image by the FFR-DG module is implemented at the beginning of the R-Net.

images effectively.

Methodology

Overview

Our $L^2RIRNet$ comprises two parts: the Pairwise Degradation Feature Vector Extraction Network (P-Net) and the Restoration Network (R-Net). As illustrated in Figure 2, the P-Net extracts the degradation feature vector from the input image, which is then constrained by the contrastive learning loss. We aim to learn the information that affects the image quality of low-light-rainy images. The P-Net encodes the degradation operator into a low-dimensional feature to guide the restoration process using a U-Net-like network.

Specifically, for the P-Net, we first calculate the fused feature P_{en} via adaptive map module, encode the P_{en} using Encoder, and then decode the latent features using Decoder:

$$\begin{aligned} Feature &= P_{Encoder}(P_{en}), \\ Latent &= P_{Decoder}(Feature). \end{aligned} \quad (1)$$

Subsequently, the R-Net uses the degradation feature vector obtained from the P-Net to guide the restoration process, which produces the output:

$$Output = R(input, Latent). \quad (2)$$

Finally, we obtain the restored image. We detail the key components below.

Pairwise Degradation Feature Vector Extraction Network (P-Net)

Adaptive Map for Low-light-rainy Images. In this section, we present a method to represent light intensity using E

and the Euclidean distance $r = \sqrt{(x_1 - x_0)^2 + (y_1 - y_0)^2}$ from surrounding pixels (x_1, y_1) to the center (x_0, y_0) of a light source. We use a real-world image of a low-light-rainy scene containing light sources as an example, as shown in Figure 3. We construct a straight line to obtain the relationship curve between E and r as $E = \frac{E_0}{r^2}$, where E_0 represents the light intensity at the center of the light source. To calculate the raindrop density m , we construct numerous 20×20 patch blocks passing through the straight line. Similarly, we construct the relationship between m and r .

The following relationships can describe the distribution of raindrops: in the region between 0 and 200, it is challenging to capture raindrop information due to overexposure near the light source; in the region between 200 and 900, raindrop information is more visible, and the degraded information is dominated by raindrop information; and in the region between 900 and infinity, capturing raindrop information is also challenging, because of the image degradation caused by the low-light condition.

In Figure 4, we utilize the attention map proposed by (Y, X, and D 2021) to highlight the image’s dark areas, allowing the network to capture the low-light degradation information. Meanwhile, by using the complement of the attention map (i.e., 1-MAP), the bright regions of the image, which correspond to the rain pattern information in those areas, can be emphasized. By training the network to process the bright and dark areas independently using the MAP and 1-MAP, we can obtain the resulting degraded quality information and effectively guide the R-Net. The P_s and P_c represent the dark and light areas of the image, respectively.

$$\begin{cases} P_s = image \otimes (1 - MAP), \\ P_c = image \otimes MAP, \end{cases} \quad (3)$$

where \otimes is the element-wise product. The P_s and P_c are

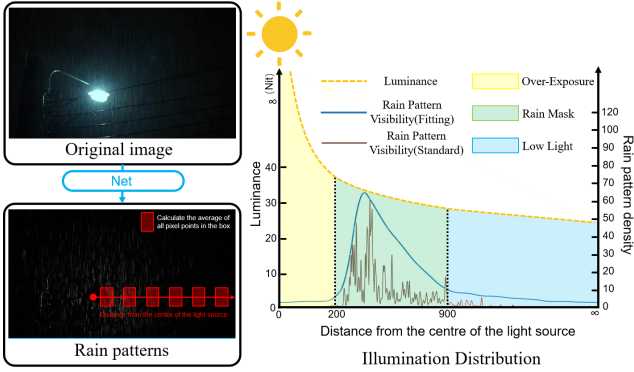


Figure 3: We choose a real-world low-light-rainy image that contains a light source. The pre-trained RCDNet obtains the rain pattern mask (Wang et al. 2023), with the light source as the center and the Euclidean distance from the ambient point to the light source as r . From the physical equation, we know that the ambient point brightness is $E = \frac{E_0}{r^2}$. We select multiple patches and calculate their rain pattern density m to get the $E - m$ curve and filter it. We can see that in the range of [200, 900], the degradation information is mainly rain pattern information, while in the range of [900, infinity], low light is the primary degradation.

concatenated as P_{en} and then fed to the Encoder of P-Net to learn features in elevated dimensions, and the multidimensional degradation feature obtained by the Decoder is later used to guide the recovery process.

Degradation Feature Vector Extraction by Effective Contrastive Learning. Using contrastive learning as the loss function can significantly improve the performance of neural networks, as demonstrated by (Wu et al. 2021). Contrastive learning can also be applied to extract information from degraded image quality, as shown by (Wang et al. 2021). In such cases, the degradation feature vector can be represented by a multiplication or addition formula.

Limitation of classic contrast learning. Degradation feature extraction is a common approach in image restoration (Wang et al. 2021; Li, Chen, and Lin 2022; Zhang, Liang, and L 2021). One of the most classic methods is the contrastive learning scheme of DASR (Wang et al. 2021), which involves choosing the positive patches from the same image as the anchor patch, and the negative patches from the paired clean image. However, our previous analysis in section reveals significant differences in the degradation feature vector across various positions of low-light-rainy images. This makes the approach unsuitable for our research. Thus, we explore alternative methods to capture degradation information effectively.

Solution. To address this limitation, instead of selecting the positive label from the same image with the anchor, we propose an alternative approach that utilizes a paired clean image x_{clean} along with the low-light-rainy image x as the negative label and its augmentation version x_{aug} as the positive label. To augment the dataset, we perform rotations of 90, 180, and 270 degrees and horizontal flipping for each

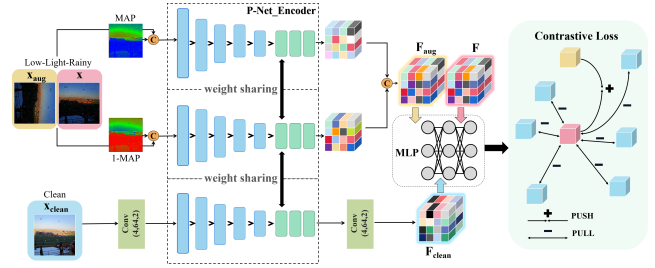


Figure 4: Constraints on degradation feature vector in the P-Net. We present the complete encoder part of the P-Net, which takes in three images: a low-light-rainy image x , an augmented version of that image x_{aug} , and a paired clean image x_{clean} . These images are encoded using a parameter-sharing network, with attention maps used to focus on the degradation feature vector in both bright and dark regions. A multilayer perceptron (MLP) then processes the resulting feature information to obtain the degradation operator for comparison learning constraint. Our approach aims to make F and F_{aug} similar while keeping F and F_{clean} distinct.

training sample. The features outputted from the P-Net encoder (P_{En}) are fed into a two-layer multi-layer perceptron (MLP) projection head to obtain three vectors. The loss function is defined as:

$$L_P = \frac{\|MLP(P_{En}(F)) - MLP(P_{En}(F_{aug}))\|_1}{\|MLP(P_{En}(F)) - MLP(P_{En}(F_{clean}))\|_1}. \quad (4)$$

We develop a novel method that learns a degradation feature vector capable of attracting “positive” pairs in a specific metric space while simultaneously pushing “negative” pairs apart. We then use the decoded degradation feature vector to generate multi-channel latent features that guide the restoration process.

P-Net Framework. In the previous sub-section, we discuss the purpose of the degradation feature vector, which is to capture the degraded information that causes a decrease in image quality. Therefore, it is essential to extract the degraded information accurately and enable effective learning of restoration networks. In the case of low-light and rainy images, degradation is mainly caused by factors such as low-light and rain streaks. Our experiments demonstrate that the degradation information of rain streaks can be better captured in the [200,900] region. In contrast, the degradation information of low light can be better captured from 900 to the edge. Based on this, we propose a novel P-Net, which can learn degradation information for bright and dark regions separately.

The P-Net is an effective network for extracting degradation information, similar in structure to the U-Net, which comprises an attention map extraction, an encoder and a decoder. Depending on the attention map, we divide the image into bright and dark regions, making the network focus more on each area during training. Specifically, we extract different degradation information from the two regions and then fuse them.

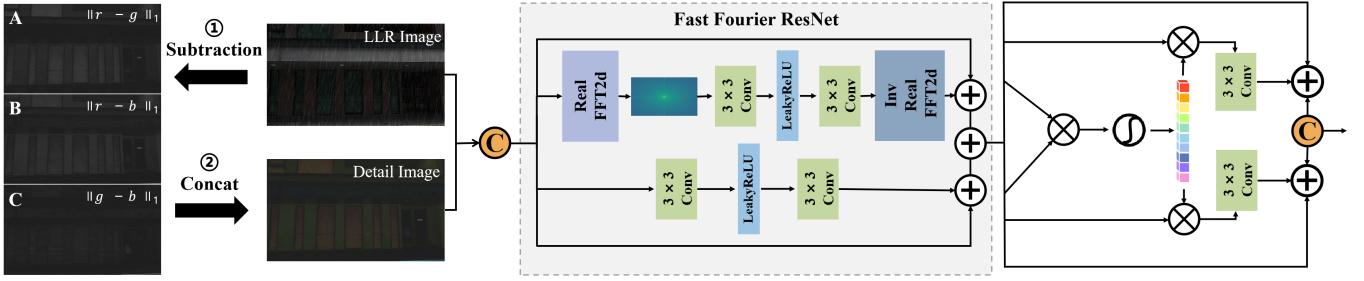


Figure 5: The architecture of the FFR-DG module is as follows. We begin by subtracting the RGB channels of a low-light-rainy (LLR) image and concatenating them to form a new detail image. Next, we feed the detail image and the LLR image into a Fast Fourier - ResNet convolution to transform them into the frequency domain. Finally, we use the resulting fusion to guide the restoration process.

Restoration Network (R-Net)

Fast Fourier - ResNet Detail Guidance Module (FFR-DG). Low illumination and noise affect not only image content but also the distribution of rain patterns, which impacts the visibility of image. Removing the rain pattern information while recovering the lighting is a challenging task. We propose an innovative Fast Fourier- ResNet Detail Guidance Module to overcome this issue and provide well-defined prior information for the restoration process. This module utilizes a detail image of the background without rain patterns as a guide during network training.

As shown in Figure 5, we can reduce the impact of rain patterns while preserving image texture in the background by subtracting channels and obtaining three single-channel maps and a concatenated detail image. This approach can be considered a preliminary rain removal strategy, and the resulting images can be effectively used for the restoration tasks. Our specific implementation includes the following steps:

$$\begin{cases} A = \|r - g\|_1, \\ B = \|r - b\|_1, \\ C = \|g - b\|_1. \end{cases} \quad (5)$$

To begin with, we extract the three channels (red, green, and blue) of the input image, denoted as r , g , and b . We then calculate the absolute differences between each pair of channels, resulting in three single-channel maps labeled A , B , and C . Next, we use these maps to concatenate a detail image, which captures the unique features of each single-layer map. This detail image is then passed to a deep FFR-DG module, along with a low-light-rainy image. The FFR-DG module has two distinct paths for processing input feature channels: a spatial path that applies conventional convolution to a subset of the channels and a frequency path that operates in the Fourier domain. The Fourier transform is a widely used tool for analyzing the frequency content of signals, including images, where the spatial variation in pixel density has a unique representation in the frequency domain. This allows for the efficient analysis and processing of images, as well as other complex signals, using Fourier-based techniques. Using element multiplication, we enhance the detail image, and then capture the resulting features to obtain prior information to guide the preliminary restoration

of the image. Our experimental results demonstrate that the proposed method effectively removes rain patterns from the image while preserving background content information. As a result, the FFR-DG module can focus on learning the background information, thereby improving its ability to remove rain pattern information.

R-Net Framework. Our R-Net architecture is specifically designed to restore low-light-rainy images to their corresponding clean versions. This is achieved through two main components: an FFR-DG module, an encoder, and a decoder.

As detailed in the previous sub-section, the FFR-DG module processes both the detail image and the low-light-rainy image, concatenating them to form the input for the encoder. This pre-processing step can reduce noise and rain pattern, preserve image details, and enhance contrast. The encoder is responsible for extracting feature information from the input image by increasing its dimension. The encoded feature information is transmitted to the decoder via a mid-level jump connection.

To enhance the accuracy of the restoration process, the decoder of R-Net utilizes the degradation feature from multiple layers by P-Net. This allows the R-Net architecture to focus more on the degraded components of the image, thereby improving the efficiency and performance of the restoration process.

We use the L1 loss and the perceptual loss for our R-Net ($R(\bullet)$). Specifically, the loss function is defined as:

$$L_R = \|R(x) - x_{clean}\|_1 + \lambda_{per} \|\Phi(R(x)) - \Phi(x_{clean})\|_1 \quad (6)$$

where $\Phi(\cdot)$ denotes the pre-trained VGG19 network and we adopt multi-scale feature maps from layer $\{conv1, \dots, conv4\}$ following the widely-used setting.

The overall loss function is:

$$L = \lambda_P L_P + \lambda_R L_R \quad (7)$$

We set the loss weights of λ_P , λ_R and λ_{per} to 1, 1 and 0.1, respectively.

Table 1: Quantitative evaluation on the LLR Dataset. The baseline contains the cascaded methods (Enhancement-Deraining and Deraining-Enhancement) and retrained methods on our LLR Dataset. ‘*’ indicates the network is retrained on our LLR Dataset. The parameters and running time are expressed in millions (M) and milliseconds (Ms) separately. All running time is evaluated on a 512×512 image using a Geforce RTX 3090.

Methods	Cascaded Methods				Training on LLR Dataset				
	Enhancement-Deraining		Deraining-Enhancement		Zero-DCE*	RCDNet*	PyDiff*	MIRNet*	$L^2 RIRNet(ours)$
Network	Zero-DCE ⇒ RCDNet	SCI ⇒ MIRNet	MIRNet ⇒ SCI	RCDNet ⇒ Zero-DCE					
PSNR(dB)	17.58	20.71	19.32	12.21	21.75	25.04	29.06	29.31	29.96
SSIM	0.6634	0.7186	0.6931	0.6175	0.7189	0.8031	0.8753	0.8872	0.9007
Params (M)	3.5	32.3	32.3	3.5	0.5	3.0	54.5	31.8	11.9
Running time (Ms)	235.33	198.5	198.5	235.33	57.806	177.52	373.56	193.5	58.384

Experiments

Proposed Dataset and Experimental Settings

Our Dataset. For detailed information about our dataset, please see the Supplementary Material. To train our $L^2 RIRNet$, we contribute an LLR Dataset by combining both synthetic and real-world images. It contains 8200 pairs of synthetic images for training, 800 synthetic images and 430 real-world images for testing. Inspired by LEDNet (Zhou, Li, and Loy 2022), we first synthesize the low-light-rainy images by decreasing the lighting intensity of synthetic rainy images from the rain dataset (Zhang and Petel 2018). We then consider the lighting distribution characteristics of real-world environments and simulate them by randomly selecting patches from the images in the first part. We enhance the pixels within these patches while reducing the lighting in other areas. At last, we collect a series of real-world images, some of which we searched in existing rainy datasets, while others are captured by ourselves. We also search for additional images on the Internet, which allows us to include real-world low-light-rainy images. These three components are combined to form our training and testing sets.

Implementation details. For our P-Net and R-Net, we utilize a U-Net-like architecture. To optimize our proposed network, we adopt the Adam optimizer algorithm with $\beta_1=0.9$, $\beta_2=0.999$, and the initial learning rate is set to 2×10^{-4} and decreases uniformly to 10^{-6} . The batch size is set to 24, the used framework is PyTorch, and the used GPU is GeForce RTX 3090. The input image is randomly cropped to 256×256 , and we train our $L^2 RIRNet$ for 200 epochs.

Evaluation Metrics. We employ the PSNR and SSIM metrics to evaluate the synthetic images in the LLR Dataset, and for better comparison, the network parameters are also given. For real-world images in the LLR Dataset, since no ground truth for calculating PSNR and SSIM, the classical non-reference NIQE (A., R., and Bovik 2012) is applied as our perceptual metrics.

Comparisons on the LLR Dataset

We evaluate the effectiveness of our proposed $L^2 RIRNet$ on the synthetic and real-world images from LLR Dataset quantitatively and qualitatively. As the joint task addressed in this paper is novel, no opened existing methods can be

directly compared with ours. To provide a comprehensive evaluation, we carefully select and combine the representative low-light enhancement and deraining methods, resulting in two distinct baseline methods for comparison: cascaded and retrained.

Cascaded Methods. For low-light enhancement networks, we choose the classic Zero-DCE (Guo et al. 2020) from CVPR 2020 and the state-of-the-art low-light enhancement network SCI (Ma et al. 2022) from CVPR 2022. For deraining, we choose two recent deraining methods: MIRNet (W et al. 2022) (TPAMI 2022) and RCDNet (Wang et al. 2023) (2023 TNNLS).

Retrained Methods. Since SCI (Ma et al. 2022) is a self-supervised network, its supervised retraining does not yield satisfactory results, so we use another recent method: Pydiff (Zhou, Yang, and Yang 2023) (IJCAI 2023) as our retrained network. For deraining, we carefully choose some state-of-the-art networks for retraining: MIRNet (W et al. 2022) (TPAMI 2022) and RCDNet (Wang et al. 2023) (2023 TNNLS).

Quantitative and Qualitative Evaluations. Table 1 reports the average PSNR and SSIM values of different state-of-the-art restoration methods on synthetic images from the LLR Dataset. The results demonstrate that our $L^2 RIRNet$ achieves the best performance among all the methods evaluated. Importantly, our approach shows a significant advantage compared to the four cascade approaches. After retraining these state-of-the-art networks on the LLR Dataset, our $L^2 RIRNet$ still outperforms them. For instance, comparing our method with that MIRNet in TPAMI 2022, there is a similar number of model parameters but obvious increases in PSNR and SSIM respectively. As shown in Table 3, the proposed $L^2 RIRNet$ achieves the lowest NIQE score, indicating that our results are perceptually best.

Figures 6 and 7 provide a visual comparison of a synthetic and real-world images from LLR Dataset. For the limited space, we only choose some of the best results of methods. Among other issues, regardless of whether it is a synthetic or real image, the results of cascade method are consistently unsatisfactory, often leaving behind rain pattern residue or overexposed. While some state-of-the-art methods show improvements after retraining on synthetic images, rain residue and partial blurring are still evident in real im-

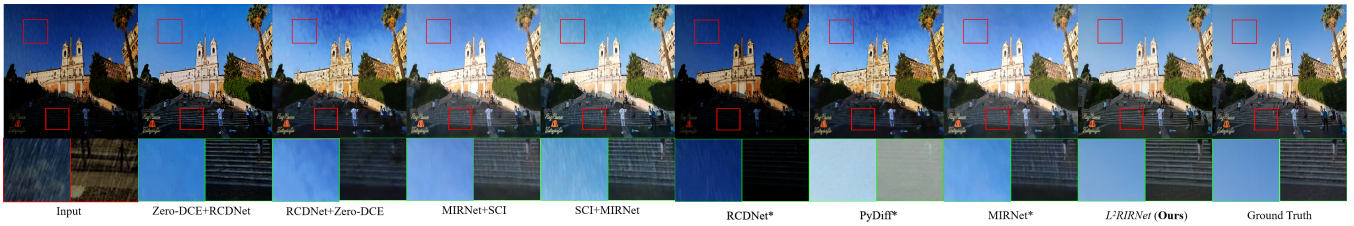


Figure 6: Visual comparison on an image from the LLR Dataset. ‘*’ indicates the network is retrained on our LLR Dataset.

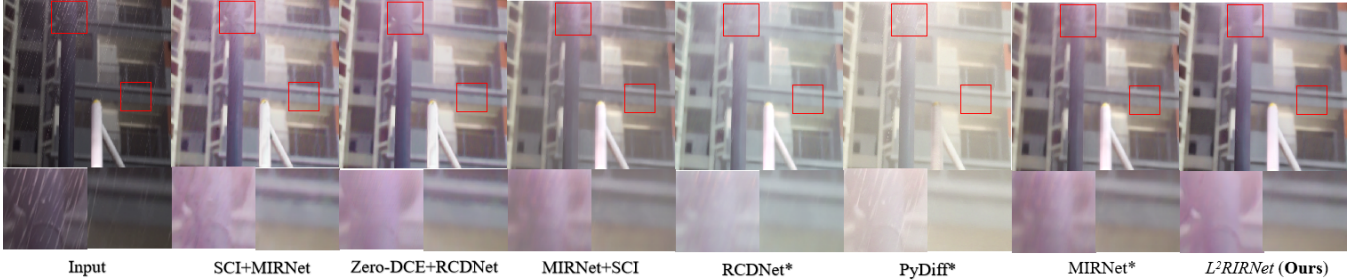


Figure 7: Visual comparison on a real-world image. ‘*’ indicates the network is retrained on our LLR Dataset.

Table 2: Quantitative evaluation on the real-world LLR Dataset.

	Input	Zero-DCE*	RCDNet*
NIQE ↓	16.927	16.155	15.943
	PyDiff*	MIRNet*	$L^2RIRNet(Ours)$
NIQE ↓	14.795	14.658	13.881

Table 3: **V1**: Only the R-Net; **V2**: R-Net + S-Net(Single branch degradation feature vector extraction network) ; **V3**: R-Net + P-Net; **V4**: Our $L^2RIRNet$.

Methods	V1	V2	V3	V4(Ours)
R-Net	✓	✓	✓	✓
S-Net		✓		
P-Net			✓	✓
FFR-DG module				✓
PSNR(dB)	28.06	28.54	29.12	29.96

ages.

Ablation Study

In this subsection, we aim to demonstrate the effectiveness of the key components of our $L^2RIRNet$ architecture. Table 3 shows four different variants of the network. V1 represents only the R-Net. V2 combines the R-Net with the Single Degradation Feature Vector Extraction Network (S-Net). V3 combines the R-Net with the P-Net. V4 represents our complete $L^2RIRNet$.

By carefully comparing these variants, we gain important insights into the performance of our $L^2RIRNet$. Comparing V1 with V2, we find that adding a degradation feature

vector can improve restoration performance. Furthermore, comparing V2 with V3, we discover that the PSNR is increased by 0.58dB. This result proves the vital role of our P-Net in extracting degradation information from both bright and dark regions using dual channels, resulting in significant improvement compared to single channels. Most importantly, when we compare V3 with V4, we find that adding the FFR-DG module results in a 0.84dB increase in PSNR. This result highlights the value of our proposed method, as it demonstrates the importance of adding prior details and Fourier frequency domain information to the restoration process. These results demonstrate the effectiveness of each key part of our $L^2RIRNet$ architecture and the importance of combining them to achieve state-of-the-art performance. Due to limited space, other ablation experiments, the specific structure of these variants and visible results are provided in the Supplementary Material.

CONCLUSION

In this paper, we present an end-to-end framework for low-light rainy image restoration that outperforms existing solutions for both synthetic and real images. As a key design, we propose a P-Net that can extract distinct degradation feature vectors for the degraded bright and dark regions, thereby accurately capturing the causes of image degradation. In addition, we introduce an FFR-DG module based on the Fourier frequency domain transformation that provides excellent detail prior guidance information for the restoration process. Our approach offers significant improvements over current methods, highlighting the effectiveness of our framework in addressing the challenges of low-light rain image restoration.

References

- A., M.; R., S.; and Bovik. 2012. Making a “completely blind” image quality analyzer. In *IEEE Signal processing letters*, 209–212.
- C., W.; W., W.; W., Y.; and J., L. 2018. Deep retinex decomposition for low-light enhancement. In *arXiv preprint*, 1808.04560.
- Fu, X.; Huang, J.; Ding, X.; Liao, Y.; and Paisley, J. 2017a. Clearing the skies: A deep network architecture for single-image rain removal. In *IEEE Transactions on Image Processing*, 2944–2956.
- Fu, X.; Huang, J.; Zeng, D.; Yue, H.; Ding, X.; and Paisley, J. 2017b. Removing rain from single images via a deep detail network. In *IEEE Conference on Computer Vision and Pattern Recognition*, 3855–3863.
- Fu, X.; Zeng, D.; Huang, Y.; Ding, X.; and Zhang, X.-P. 2013. A variational framework for single low light image enhancement using bright channel prior. In *IEEE global conference on signal and information processing*, 1085–1088.
- Guo, C.; Li, C.; Guo, J.; Loy, C. C.; Hou, J.; Kwong, S.; and Cong, R. 2020. Zero-reference deep curve estimation for low-light image enhancement. In *Proceedings of the IEEE/CVF Conference on Computer Vision and Pattern Recognition*, 1780–1789.
- Guo, X.; Yu, L.; and Ling, H. 2016. Lime: Low-light image enhancement via illumination map estimation. In *IEEE Transactions on Image Processing*.
- Jing, X.; Wei, Z.; Peng, L.; and Tang., X. 2012. Removing rain and snow in a single image using guided filter. In *IEEE International Conference on Computer Science and Automation Engineering*.
- Jobson, D. 2004. Retinex processing for automatic image enhancement. In *Journal of Electronic Imaging*.
- Kim, J. H.; Lee, C.; Sim, J. Y.; and Kim, C. S. 2014. Single-image deraining using an adaptive nonlocal means filter. In *IEEE International Conference on Image Processing*.
- Li, C.; Guo, C.; and Loy, C. C. 2021. Learning to enhance low-light image via zero-reference deep curve estimation. In *IEEE Transactions on Pattern Analysis and Machine Intelligence*, 4225–4238.
- Li, X.; Chen, C.; and Lin, X. 2022. From Face to Natural Image: Learning Real Degradation for Blind Image Super-Resolution. In *Computer Vision–ECCV 2022: 17th European Conference*, 376–392.
- Ma, L.; Ma, T.; Liu, R.; Fan, X.; and Luo, Z. 2022. Toward Fast, Flexible, and Robust Low-Light Image Enhancement. In *Proceedings of the IEEE/CVF Conference on Computer Vision and Pattern Recognition*, 5637–5646.
- Rahman, Z.-U.; Jobson, D.; and Woodell, G. 1996. A multiscale retinex for color rendition and dynamic range compression. In *Proc. SPIE*, 183–191.
- W, Z. S.; A, A.; S, K.; M., H.; S., K. F.; H., Y. M.; and Shao, L. 2022. Learning enriched features for fast image restoration and enhancement. In *IEEE transactions on pattern analysis and machine intelligence*.
- Wang, H.; Xie, Q.; Zhao, Q.; Li, Y.; Liang, Y.; Zheng, Y.; and Meng, D. 2023. RCDNet: An interpretable rain convolutional dictionary network for single image deraining. In *IEEE Transactions on Neural Networks and Learning Systems*.
- Wang, L.; Wang, Y.; Dong, X.; Xu, Q.; Yang, J.; An, W.; and Guo, Y. 2021. Unsupervised Degradation Representation Learning for Blind Super-Resolution. In *IEEE Conference on Computer Vision and Pattern Recognition*, 10581–10590.
- Wei, Y.; Zhang, Z.; Xu, M.; Hong, R.; Fan, J.; and Yan, S. 2022a. Robust attention deraining network for synchronous rain streaks and raindrops removal. In *ACM International Conference on Multimedia*, 6464–6472.
- Wei, Y.; Zhang, Z.; Zheng, H.; Hong, R.; Yang, Y.; and Wang, M. 2022b. SGINet: Toward sufficient interaction between single image deraining and semantic segmentation. In *ACM International Conference on Multimedia*, 6202–6210.
- Wu, H.; Qu, Y.; Lin, S.; Zhou, J.; Qiao, R.; Zhang, Z.; Xie, Y.; and Ma, L. 2021. Contrastive Learning for Compact Single Image Dehazing. In *IEEE Conference on Computer Vision and Pattern Recognition*, 10551–10560.
- Y, J.; X, G.; and D, L. 2021. Enlightengan: Deep light enhancement without paired supervision. In *IEEE transactions on image processing*, 2340–2349.
- Zhang, H.; and Petel, V. M. 2018. Density-aware single image de-raining using a multi-stream dense network. In *Proceedings of the IEEE conference on computer vision and pattern recognition*, 695–704.
- Zhang, K.; Liang, J.; and L, V. G. 2021. Designing a practical degradation model for deep blind image super-resolution. In *Proceedings of the IEEE/CVF International Conference on Computer Vision*, 4791–4800.
- Zhang, Y.; Zhang, J.; and Guo, X. 2019. Kindling the darkness: A practical low-light image enhancer. In *Proceedings of the 27th ACM international conference on multimedia*, 1632–1640.
- Zheng, X.; Liao, Y.; W. Guo, X. F.; and Ding., X. 2013. Single-image-based rain and snow removal using multi-guided filter. In *International Conference on Neural Information Processing*.
- Zhihong, W.; and Xiaohong, X. 2011. Study on histogram equalization. In *Intelligence Information Processing and Trusted Computing, International Symposium on IEEE Computer Society*, 177–179.
- Zhou, D.; Yang, Z.; and Yang, Y. 2023. Pyramid Diffusion Models For Low-light Image Enhancement. In *IJCAI*.
- Zhou, S.; Li, C.; and Loy, C. C. 2022. Lednet: Joint low-light enhancement and deblurring in the dark. In *Computer Vision–ECCV 2022: 17th European Conference*.